OXFORD

JNCI J Natl Cancer Inst (2017) 109(11): djx066

doi: 10.1093/jnci/djx066
First published online May 22, 2017
Article

ARTICLE

Tumor Microvessel Density as a Potential Predictive Marker for Bevacizumab Benefit: GOG-0218 Biomarker Analyses

Carlos Bais, Barbara Mueller, Mark F. Brady, Robert S. Mannel, Robert A. Burger, Wei Wei, Koen M. Marien, Mark M. Kockx, Amreen Husain, Michael J. Birrer; on behalf of the NRG Oncology/Gynecologic Oncology Group

Affiliations of authors: Genentech Inc., South San Francisco, CA (CB – affiliation when this work was performed, AH); F Hoffmann-La Roche Ltd, Basel, Switzerland (BM); NRG Statistical and Data Center, Roswell Park Cancer Institute, Buffalo, NY (MFB); University of Oklahoma, Oklahoma City, OK (RSM); Department of Obstetrics and Gynecology, Division of Gynecologic Oncology, University of Pennsylvania, Philadelphia, PA (RAB); Center for Cancer Research, Gillette Center for Gynecologic Oncology, Massachusetts General Hospital, Harvard Medical School, Boston, MA (WW, MJB); HistoGeneX NV, Antwerp, Belgium (KMM, MMK); Division of Physiopharmacology, University of Antwerp, Antwerp, Belgium (KMM).

Correspondence to: Carlos Bais, PhD, 1 Medimmune Way, Gaithersburg, MD 20878 (e-mail: baiscarlos@gmail.com); or Michael J Birrer, MD, PhD, Center for Cancer Research, Gillette Center for Gynecologic Oncology, Massachusetts General Hospital, Harvard Medical School, Boston, MA (e-mail: mbirrer@mgh.harvard.edu).

Abstract

Background: Combining bevacizumab with frontline chemotherapy statistically significantly improved progression-free survival (PFS) but not overall survival (OS) in the phase III GOG-0218 trial. Evaluation of candidate biomarkers was an exploratory objective.

Methods: Patients with stage III (incompletely resected) or IV ovarian cancer were randomly assigned to receive six chemotherapy cycles with placebo or bevacizumab followed by single-agent placebo or bevacizumab. Five candidate tumor biomarkers were assessed by immunohistochemistry. The biomarker-evaluable population was categorized into high or low biomarker-expressing subgroups using median and quartile cutoffs. Associations between biomarker expression and efficacy were analyzed. All statistical tests were two-sided.

Results: The biomarker-evaluable population (n = 980) comprising 78.5% of the intent-to-treat population had representative baseline characteristics and efficacy outcomes. Neither prognostic nor predictive associations were seen for vascular endothelial growth factor (VEGF) receptor–2, neuropilin-1, or MET. Higher microvessel density (MVD; measured by CD31) showed predictive value for PFS (hazard ratio [HR] for bevacizumab vs placebo = 0.40, 95% confidence interval [CI] = 0.29 to 0.54, vs 0.80, 95% CI = 0.59 to 1.07, for high vs low MVD, respectively, $P_{interaction} = .003$) and OS (HR = 0.67, 95% CI = 0.51 to 0.88, vs 1.10, 95% CI = 0.84 to 1.44, $P_{interaction} = .02$). Tumor VEGF-A was not predictive for PFS but showed potential predictive value for OS using a third-quartile cutoff for high VEGF-A expression.

Conclusions: These retrospective tumor biomarker analyses suggest a positive association between density of vascular endothelial cells (the predominant cell type expressing VEGF receptors) and tumor VEGF-A levels and magnitude of bevacizumab effect in ovarian cancer. The potential predictive value of MVD (CD31) and tumor VEGF-A is consistent with a mechanism of action driven by VEGF-A signaling blockade.

Received: November 14, 2016; **Revised:** February 25, 2017; **Accepted:** March 15, 2017

Vascular endothelial growth factor (VEGF)–A, a dimeric glycoprotein, is a survival factor for endothelial cells, is considered to be a primary inducer of angiogenesis and vascular permeability, and is the molecular target of bevacizumab (1). VEGF-A mediates its effects primarily by activating VEGF receptor (VEGFR)–2, a vascular endothelial-specific tyrosine kinase receptor (2). Although VEGF-A inhibition is lethal during embryonic development (3), its neutralization is well tolerated in adults, consistent with postnatal vascular maturation and differentiation in various tissues (4). Most tumors overexpress VEGF-A, and tumor neo-vasculature is particularly sensitive to VEGF-A deprivation (4). Following demonstration that VEGF-A signaling blockade inhibits angiogenesis and tumor growth in preclinical models (4), the humanized VEGF-blocking antibody bevacizumab was evaluated in clinical trials and subsequently approved as treatment for several advanced cancers (5,6).

The Gynecologic Oncology Group (GOG)-0218 randomized phase III trial demonstrated statistically significantly improved progression-free survival (PFS) with bevacizumab added to standard frontline chemotherapy for epithelial ovarian cancer (7). These results, supported by findings from the randomized phase III ICON7 trial (8), led to European approval of frontline bevacizumab combined with chemotherapy for epithelial ovarian cancer. However, neither trial demonstrated a statistically significant effect on overall survival (OS). In GOG-0218, extensive crossover from the chemotherapy-alone arm to bevacizumab and further uncontrolled treatment lines may have masked a potential effect on OS (7,9). The present analyses explored whether candidate tumor biomarkers might define subsets of patients with epithelial ovarian cancer deriving differential clinical benefit from frontline bevacizumab.

Evaluation of potential biomarkers in prospectively collected specimens was an exploratory objective of GOG-0218. Five tumor (t) biomarkers (tVEGF-A, tVEGFR-2, neuropilin-1, MET [hepatocyte growth factor receptor], and cluster of differentiation 31 [CD31]), each supported by a biologic rationale, were assessed by immunohistochemistry (IHC). As bevacizumab targets VEGF-A, it was postulated that high tVEGF-A expression may be associated with enhanced benefit from bevacizumab. Similarly, tVEGFR-2 and neuropilin-1 (a co-receptor of VEGF-A) are logical candidates. Retrospective biomarker analyses in metastatic breast cancer suggested that low levels of neuropilin-1 may predict increased PFS benefit from bevacizumab (10). MET is biologically interesting as a candidate biomarker for bevacizumab efficacy because of its potential involvement in anti-VEGF-A resistance (11).

CD31 is an integral membrane glycoprotein expressed at high levels on endothelial cells, which form microvessels in normal tissue and tumors (12). Microvessel density (MVD) quantified based on CD31-positive endothelial cells in tumor samples assayed by IHC is often used as a surrogate for tumoral angiogenic activity (13). Higher tumoral MVD is associated with worse prognosis in several tumor types, including ovarian cancer (14–22). New, immature blood vessels within the microvasculature require VEGF-A signaling for survival, and thus are among the direct targets of bevacizumab (23). It was proposed that high MVD (measured by CD31-positive vessels/mm^2 as a possible surrogate marker of angiogenic activity and/or dependency) may be associated with greater benefit from bevacizumab (24). Retrospective analyses in colorectal cancer were consistent with this hypothesis (25), but others failed to show a relationship between MVD and bevacizumab benefit (26,27). Whether the lack of correlation reflects small patient numbers, tumor diversity, or other factors remains to be established. In this biomarker substudy of the GOG-0218 trial evaluating bevacizumab in ovarian cancer, we sought to explore the potential prognostic and predictive effects of these five tumor markers.

Methods

Study Design

In this double-blind placebo-controlled randomized phase III trial ClinicalTrials.gov number NCT00262847 (28), eligible patients had International Federation of Gynecology and Obstetrics (FIGO) (29) stage III (incompletely resected) or stage IV epithelial ovarian, primary peritoneal, or fallopian tube cancer and had undergone standard abdominal surgery with maximal debulking effort within 12 weeks preceding study entry. The study design details have been published previously (7). All patients received six cycles of carboplatin plus paclitaxel and were randomly assigned to receive: placebo during cycles 2 to 22 (chemotherapy alone); bevacizumab 15 mg/kg every three weeks during cycles 2 to 6 followed by placebo during cycles 7 to 22 (concurrent bevacizumab); or bevacizumab throughout cycles 2 to 22 (extended bevacizumab). The primary end point was PFS; OS was a secondary end point. The protocol was approved by the relevant institutional review boards or ethics committees; all patients gave written informed consent.

Biomarker Analyses

Candidate biomarkers were measured after completion of the clinical trial using paraffin-embedded formalin-fixed sections taken from the pretreatment tumor samples. The specimens for biomarker analysis were provided from the GOG tissue bank according to standard National Cancer Institute (NCI) banking material transfer agreements. All slides were sent to a single central Clinical Laboratory Improvement Amendments-certified research laboratory (HistoGeneX, Antwerp, Belgium) accredited by the College of American Pathologists and the Belgian Accreditation Organization (ISO 15189). Membrane and cytoplasmic IHC staining were undertaken using validated, fit-for-purpose assays. Sections were stained using 3,3′-diaminobenzidine for neuropilin-1 (clone C-19; Santa Cruz Biotechnology, Heidelberg, Germany), tVEGF-A (clone SP28; Abcam, Cambridge, United Kingdom), and tVEGFR-2 (clone 55B11; Cell Signaling Technology, Leiden, the Netherlands) on the Lab Vision Autostainer (ThermoFisher Scientific, Gent, Belgium), whereas CD31 (clone 1A10; Leica Biosystems, Diegem, Belgium) and cMET (clone SP44; Ventana, Basel, Switzerland) were stained using the Benchmark XT (Ventana, Basel, Switzerland). Whole-slide images were created with a Pannoramic SCAN digital slide scanner (3DHISTECH Ltd, Budapest, Hungary) using a Zeiss plan-apochromatic objective (magnification: 20x; numerical aperture: 0.8) and a Hitachi (HV-F22CL) 3CCD progressive scan color camera (resolution: 0.2325 μm/pixel). JPEG image encoding with quality factor 80 and an interpolated focus distance of 15 with stitching in the scan options was chosen. For every slide, a specific scan profile was configured and holes in the scan area were filled to allow for correct detection of tissue and in-focus images of the tissue. Scanned images were examined in Pannoramic Viewer (3DHISTECH) to check image quality and confirm that the whole tissue section was captured (30).

Microscopic analysis of the digitized slides was performed by a small number of highly experienced research pathologists and imaging scientists using rigorous research protocols. This included

ARTICLE

systematic, uniform, random sampling of at least three but generally 10 regions of interest (ROIs) from the whole-slide image to take into account potential tumor heterogeneity of the marker. An unbiased, rectangular counting grid and optimized counting rules were used for MVD quantification (Supplementary Figure 1, available online) (30,31). The pathologists and imaging scientists were blinded to clinical outcomes in the study patients. For tVEGF-A scoring, 100 cells were scored per ROI (≥10 ROIs for large tissue samples). Each cell was assigned a staining intensity: 0 (none), 1+ (weak), 2+ (intermediate), or 3+ (strong). The final histological score (H-Score) was a composite of the staining intensity for each of the 100 cells, ranging from 0 (0 in all 100 cells) to 300 (3+ in all 100 cells).

Statistical Analysis

The data cutoffs were September 29, 2009 (PFS), and August 26, 2011 (OS). The biomarker-evaluable IHC (BEI) population comprised all patients with an evaluable baseline IHC biomarker sample who received trial treatment at cycle 2 or beyond. Initially, the BEI population was dichotomized using the median value for each marker as the cutoff between low and high expression of each marker. The median was prespecified as the cutoff before performing the present biomarker analyses but after unblinding of the clinical trial results. Associations between tumor biomarker expression levels and PFS and OS were analyzed. Biomarkers showing potential predictive effect using the median as the cutoff were evaluated further to explore the effect of choosing the first or third quartile instead of the median as the cutoff to define low vs high expression of each marker. Finally, sliding window analyses were performed to explore the effect of varying cutoffs for potentially predictive biomarkers. These graphs plot the point estimate and 95% confidence interval (CI) of the treatment hazard ratio (HR) for PFS and OS for only those patients whose biomarker value falls within a window spanning 25%, which is moved in 5% steps across the entire range of possible cutoff values.

In the biomarker analyses reported here, investigator-assessed PFS and OS were calculated from the date of random assignment. PFS was censored if nonstudy therapy was initiated for any reason before disease progression or if progression was defined by cancer antigen-125 elevation alone (without Response Evaluation Criteria in Solid Tumors-defined progression). Comparisons were based on the extended bevacizumab arm vs the chemotherapy-alone arm because PFS was improved only with extended bevacizumab in the primary analysis of the intent-to-treat (ITT) population.

Two-sided treatment-by-biomarker $P_{interaction}$ values were calculated using a Cox model including treatment, biomarker (using first quartile, median, or third quartile cutoffs to define low and high biomarker expression levels), interaction of treatment by biomarker, FIGO stage and debulking status, and baseline GOG performance status. Because of the exploratory nature of the analyses, no cutoff for statistical significance is specified and no adjustment for multiple testing was performed. The assumption of proportionality was not tested for the retrospective biomarker analyses. Statistical analyses were performed by F Hoffmann-La Roche Ltd.

Results

Patient Population

The BEI population included 980 (78.5%) of the 1248 patients randomly assigned to either placebo or extended bevacizumab (Figure 1). Baseline characteristics in the BEI and ITT populations were similar, indicating that the BEI population was a representative subset of the ITT population (Table 1). Furthermore, efficacy outcomes were similar in the BEI and ITT populations. In the control arm, median PFS was 12.1 months (95% confidence interval [CI] = 10.6 to 12.7 months) in the BEI population (n = 483) vs 12.0 months (95% CI = 10.4 to 12.5 months) in the ITT population (n = 625) (Supplementary Figure 2, available online). In the extended bevacizumab arm, median PFS was 18.7 months (95% CI = 16.3 to 20.6 months) and 18.2 months (95% CI = 16.1 to 19.7 months) in the BEI (n = 497) and ITT (n = 623) populations, respectively. The stratified hazard ratio for PFS was 0.61 (95% CI = 0.49 to 0.74) in the BEI population and 0.62 (95% CI = 0.52 to 0.75) in the ITT population (Supplementary Figure 2, available online). A similar pattern was seen for OS: stratified hazard ratios were 0.86 (95% CI = 0.72 to 1.04) vs 0.88 (95% CI = 0.75 to 1.04) in the BEI and ITT populations, respectively (32).

MET, Neuropilin-1, and tVEGFR-2

Analyses of PFS and OS using the median as the cutoff between low and high biomarker subgroups showed no association with bevacizumab treatment effect for MET, neuropilin-1, or tVEGFR-2 (Figure 2). None of the markers appeared to be prognostic for PFS or OS, as indicated by the similar median values in high and low subgroups in the control arm.

MVD (CD31)

The number of CD31-positive vessels/mm^2 of tumor tissue was used to indicate MVD. The effect of bevacizumab on both PFS and OS was greater in patients with higher (above median) MVD. For PFS, the hazard ratio was 0.40 (95% CI = 0.29 to 0.54) favoring bevacizumab in the high MVD subgroup vs 0.80 (95% CI = 0.59 to 1.07) in patients with low MVD ($P_{interaction}$ = .003) (Figure 2A and Figure 3A). The OS hazard ratios were 0.67 (95% CI = 0.51 to 0.88) vs 1.10 (95% CI = 0.84 to 1.44), respectively ($P_{interaction}$ = .02) (Figure 2B and Figure 3B). The $P_{interaction}$ values suggest that MVD is predictive for bevacizumab treatment effect.

Supplementary Figure 3 (available online) shows the distribution of MVD across the BEI population. The potential predictive value of MVD for OS appeared to be greater using the third quartile as the cutoff to define high vs low MVD (Figure 4). Sliding window analyses supported these observations, suggesting increasing magnitude of both PFS and OS benefits from bevacizumab with increasing MVD (Supplementary Figure 4, available online).

In the control arm, patients with high MVD had worse outcomes than those with low MVD, suggesting a prognostic effect of MVD for both PFS and OS (Figure 3).

tVEGF-A

In contrast to MVD, no differential treatment effect on PFS was observed in subgroup analyses according to tVEGF-A expression dichotomized at the median (HR = 0.57, 95% CI = 0.42 to 0.75, vs HR = 0.62, 95% CI = 0.45 to 0.86, in those with high vs low tVEGF-A expression, $P_{interaction}$ = .75) (Figure 2A). For OS, there was a suggestion of a greater bevacizumab treatment effect in patients with high tVEGF-A expression (HR = 0.72, 95% CI = 0.56 to 0.94, vs HR = 1.06, 95% CI = 0.81 to 1.39, for high vs low tVEGF-A, $P_{interaction}$ = .06) (Figure 2B). As with MVD, the potential

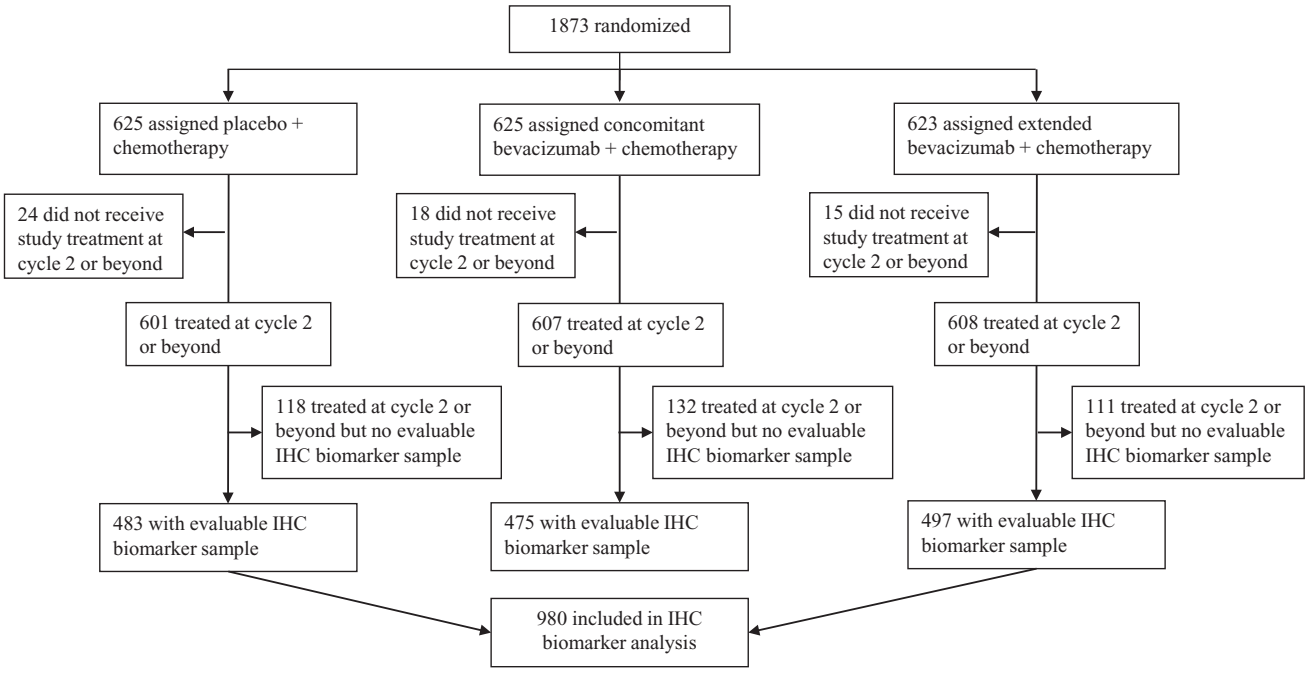

Figure 1. Trial profile. IHC = immunohistochemistry.

Table 1. Baseline characteristics in the biomarker-evaluable immunohistochemistry and intention-to-treat populations*

Characteristic	BEI population		ITT population	
	Placebo + chemotherapy (n = 483)	Extended bevacizumab + chemotherapy (n = 497)	Placebo + chemotherapy (n = 625)	Extended bevacizumab + chemotherapy (n = 623)
Median age (range), y	60 (26 to 85)	59 (22 to 89)	60 (24 to 85)	59 (22 to 89)
GOG performance status, No. (%)				
0	237 (49.1)	250 (50.3)	311 (49.8)	307 (49.3)
1/2	246 (50.9)	247 (49.7)	314 (50.2)	316 (50.7)
Primary disease site: ovary, No. (%)	398 (82.4)	419 (84.3)	515 (82.4)	531 (85.2)
FIGO stage and debulking status at diagnosis, No. (%)				
III optimally debulked	161 (33.3)	171 (34.4)	219 (35.0)	216 (34.7)
III suboptimally debulked	203 (42.0)	194 (39.0)	253 (40.5)	242 (38.8)
IV	119 (24.6)	132 (26.6)	153 (24.5)	165 (26.5)
Mucinous or clear cell, No. (%)	20 (4.1)	28 (5.6)	Clear cell 20 (3.2) Mucinous 11 (1.8)	Clear cell 25 (4.0) Mucinous 10 (1.6)
Mean residuum (SD), cm	2.7 (3.68)	2.6 (3.65)	2.6 (3.49)	2.7 (3.77)
Ascites present at baseline, No. (%)	347 (71.8)	353 (71.0)	454 (72.6)	445 (71.4)
Measurable disease at baseline, No. (%)	321 (66.4)	314 (63.2)	396 (63.4)	403 (64.7)

*BEI = biomarker-evaluable immunohistochemistry; FIGO = International Federation of Gynecology and Obstetrics; ITT = intention-to-treat.

predictive effect of tVEGF-A on OS was greater using the third quartile as the cutoff between high and low tVEGF-A expression (HR = 0.61, 95% CI = 0.42 to 0.89, vs HR = 1.00, 95% CI = 0.80 to 1.23, respectively, $P_{interaction}$ = .02) (Figure 5).

Sliding window analyses suggested that the highest percentile was associated with the largest PFS improvement with bevacizumab (Supplementary Figure 4, available online). For OS, there was a more clearly detectable pattern of increasing OS benefit from bevacizumab with increasing tVEGF-A expression. The histogram showing the distribution of tVEGF-A expression levels across the GOG-0218 BEI population had a long tail to the right (Supplementary Figure 5, available online), indicating that a relatively small subset of patients expressed extremely high levels of tVEGF-A.

ARTICLE

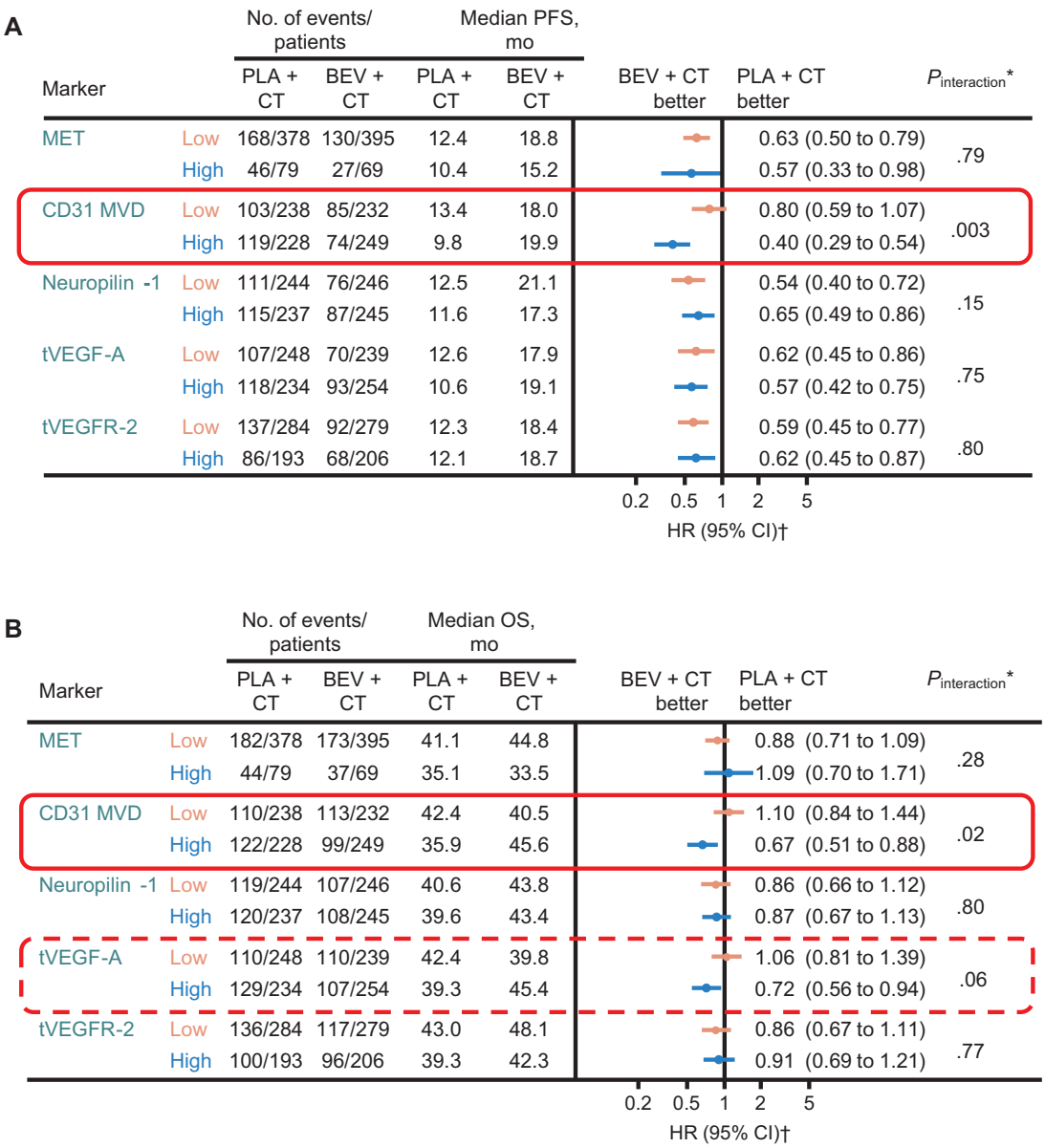

Figure 2. Overview of candidate biomarkers for **(A)** progression-free survival and **(B)** overall survival.

*Cox model including treatment, biomarker (dichotomized at median), interaction of treatment by biomarker, International Federation of Gynecology and Obstetrics (FIGO) stage and debulking status, and baseline performance status as covariates. The two-sided interaction test was performed using the Wald test. †Stratified analysis (using the two stratification factors used for patient random assignment: FIGO stage and debulking status, and baseline performance status). BEV = bevacizumab; CD = cluster of differentiation; CI = confidence interval; CT = chemotherapy; HR = hazard ratio; MVD = microvessel density; OS = overall survival; PFS = progression-free survival; PLA = placebo; tVEGF = tumor vascular endothelial growth factor; tVEGFR = tumor vascular endothelial growth factor receptor.

In the control arm, high tVEGF-A expression appeared to be associated with worse PFS outcome, but the prognostic effect of tVEGF-A on OS was less consistent (Figure 5).

Discussion

These retrospective tumor biomarker analyses suggest a positive association between the density of vascular endothelial cells (the predominant cell type expressing VEGF receptors) and tVEGF-A levels and the magnitude of OS improvement from frontline bevacizumab in epithelial ovarian cancer (and PFS improvement for MVD). In analyses according to MVD levels, improvement in PFS (primary end point) with the addition of bevacizumab to chemotherapy was seen in both the subgroup with high (above median) MVD and the subgroup with low MVD. However, the extent of PFS benefit was markedly more pronounced in patients with higher MVD. In the subgroup of patients with higher MVD, there was also an OS gain, contrasting with the lack of OS benefit observed in the ITT population. There was no OS effect of bevacizumab (either beneficial or detrimental) in patients with low MVD. There was also a suggestion of OS improvement with bevacizumab in patients with high tVEGF-A expression, although such an effect was not observed for PFS. The remaining three tumor markers evaluated (MET, neuropilin-1, and tVEGFR-2) showed no predictive value for bevacizumab efficacy.

ARTICLE

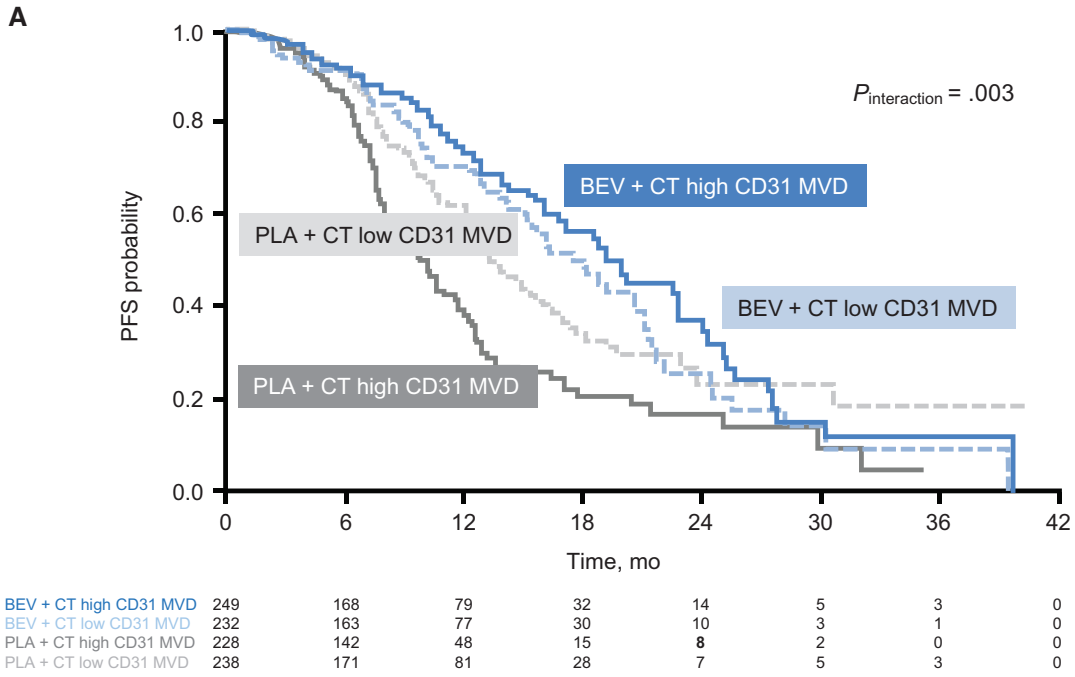

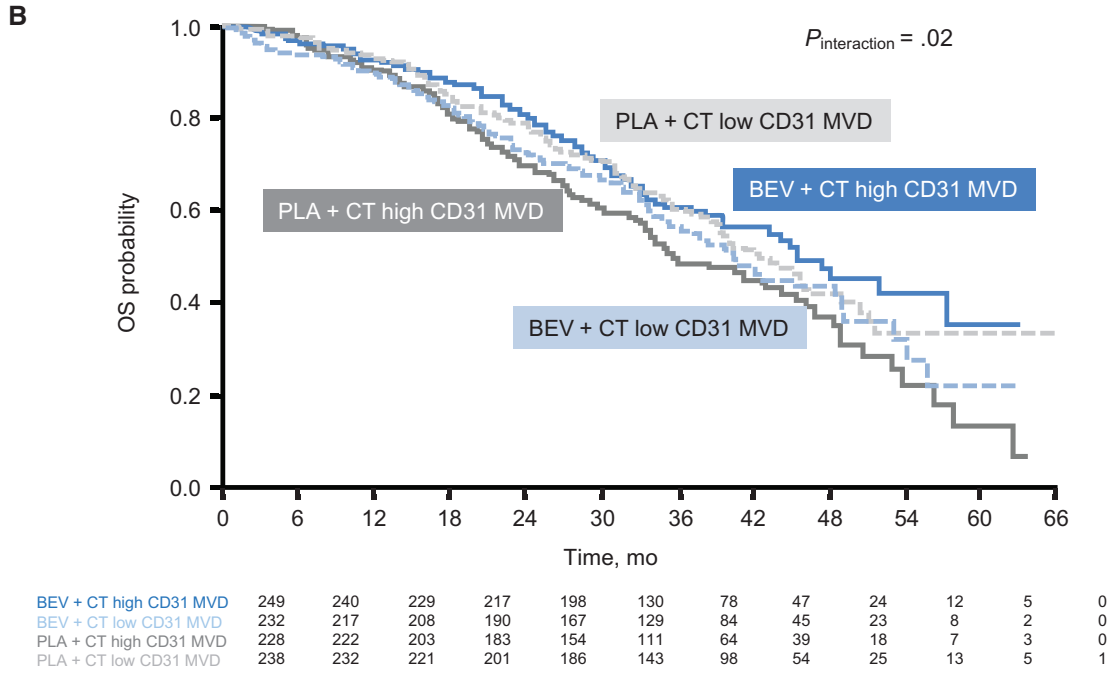

Figure 3. Relationship between microvessel density and outcome (median cutoff). **A)** Progression-free survival and **(B)** overall survival are shown. The two-sided interaction test was performed using the Wald test. BEV = bevacizumab; CD = cluster of differentiation; CT = chemotherapy; MVD = microvessel density; OS = overall survival; PFS = progression-free survival; PLA = placebo.

The main limitation of these analyses is their retrospective and exploratory nature. One of the strengths of this analysis is the very large sample size (n = 980), the high proportion of patients (78.5%) with samples available for translational research, and the high quality of the specimens. Importantly, the BEI population was representative of the ITT population, showing similar baseline characteristics and efficacy outcomes. This contrasts with previously reported biomarker analyses of the ICON7 trial, which used smaller subsets of samples (33–36). The association between higher levels of MVD and the molecular target of anti-VEGF therapy and enhanced benefit from bevacizumab is consistent with one of the postulated mechanisms

A

Cutoff		No. of events/patients PLA + CT	No. of events/patients BEV + CT	Median PFS, mo PLA + CT	Median PFS, mo BEV + CT	BEV + CT better / PLA + CT better	$P_{interaction}$*
BEI		226/483	164/497	12.1	18.7	0.61 (0.49 to 0.74)	
Q1	Low	57/124	48/123	13.1	18.8	0.70 (0.47 to 1.05)	.20
	High	165/342	111/358	11.0	18.7	0.54 (0.42 to 0.69)	
Median	Low	103/238	85/232	13.4	18.0	0.80 (0.59 to 1.07)	.003
	High	119/228	74/249	9.8	19.9	0.40 (0.29 to 0.54)	
Q3	Low	160/355	121/351	12.5	18.8	0.67 (0.53 to 0.86)	.03
	High	62/111	38/130	10.2	18.7	0.37 (0.24 to 0.56)	

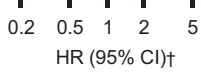

B

Cutoff		No. of events/patients PLA + CT	No. of events/patients BEV + CT	Median OS, mo PLA + CT	Median OS, mo BEV + CT	BEV + CT better / PLA + CT better	$P_{interaction}$*
BEI		240/483	217/497	40.2	43.8	0.86 (0.72 to 1.04)	
Q1	Low	60/124	59/123	43.3	40.6	0.95 (0.66 to 1.36)	.50
	High	172/342	153/358	39.4	44.8	0.84 (0.67 to 1.05)	
Median	Low	110/238	113/232	42.4	40.5	1.10 (0.84 to 1.44)	.02
	High	122/228	99/249	35.9	45.6	0.67 (0.51 to 0.88)	
Q3	Low	169/355	165/351	41.5	42.1	1.03 (0.83 to 1.27)	.008
	High	63/111	47/130	34.1	45.6	0.56 (0.38 to 0.83)	

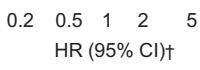

C

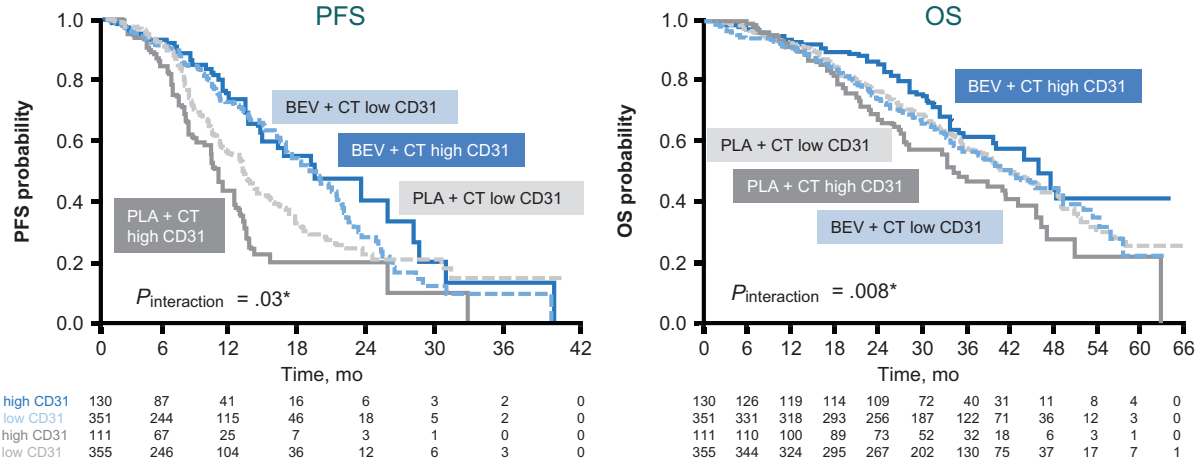

BEV + CT high CD31	130	87	41	16	6	3	2	0
BEV + CT low CD31	351	244	115	46	18	5	2	0
PLA + CT high CD31	111	67	25	7	3	1	0	0
PLA + CT low CD31	355	246	104	36	12	6	3	0

130	126	119	114	109	72	40	31	11	8	4	0		
351	331	318	293	256	187	122	71	36	12	3	0		
111	110	100	89	73	52	32	18	6	3	1	0		
355	344	324	295	267	202	130	75	37	17	7	1		

Figure 4. Microvessel density (MVD) analyses by quartile. **A)** Progression-free survival (PFS) by CD31 MVD quartile. **B)** Overall survival (OS) by MVD quartile. **C)** PFS and OS by MVD using Q3 as the cutoff. The two-sided interaction test was performed using the Wald test. *Cox model including treatment, biomarker (dichotomized at quartile 1, median, or quartile 3), interaction of treatment by biomarker, International Federation of Gynecology and Obstetrics (FIGO) stage and debulking status, and baseline performance status as covariates. †Stratified analyses (using the two stratification factors used for patient random assignment: FIGO stage and debulking status, and baseline performance status). BEI = biomarker-evaluable immunohistochemistry; BEV = bevacizumab; CD = cluster of differentiation; CI = confidence interval; CT = chemotherapy; HR = hazard ratio; OS = overall survival; PFS = progression-free survival; PLA = placebo; Q = quartile.

ARTICLE

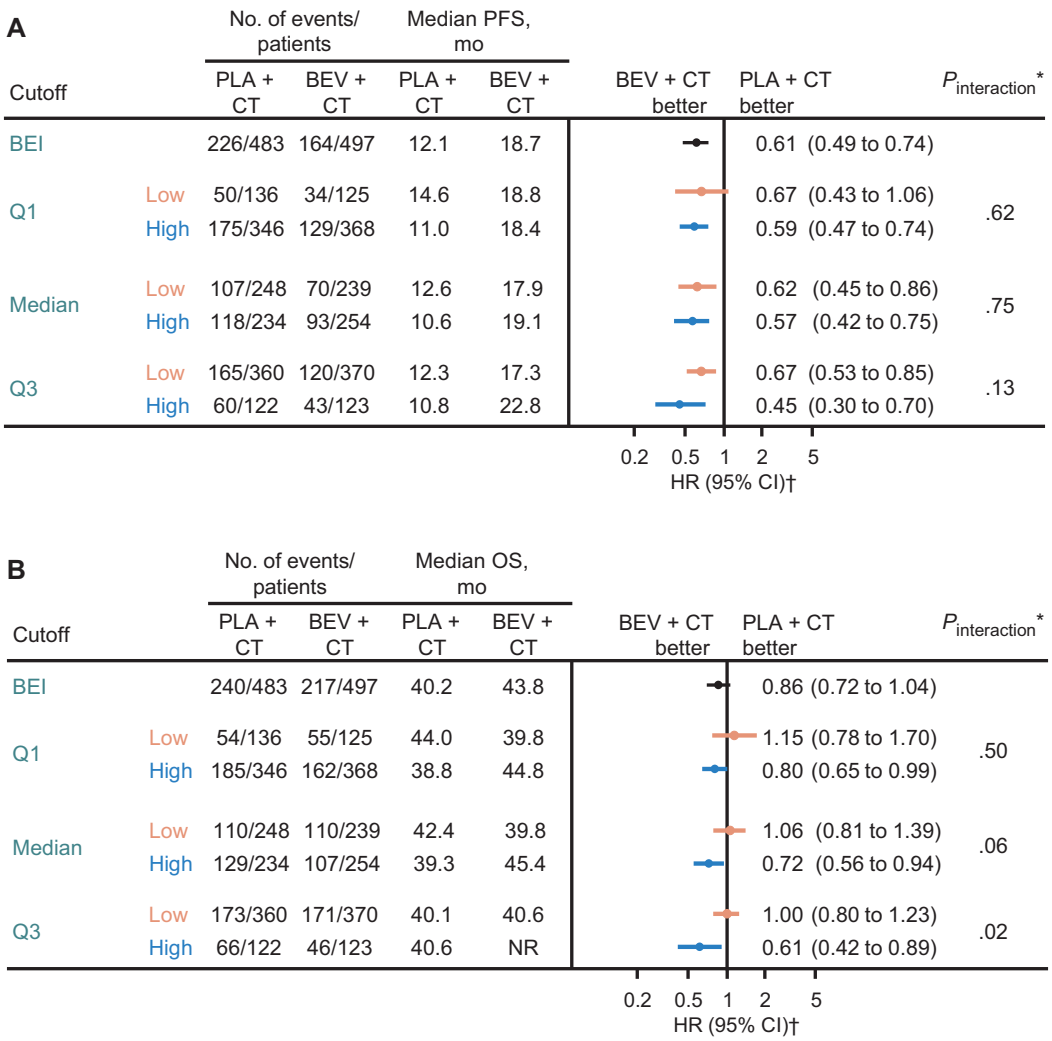

Figure 5. Bevacizumab treatment effect by tumor vascular endothelial growth factor–A quartile. **A)** Progression-free survival. **B)** Overall survival. The two-sided interaction test was performed using the Wald test. *Cox model including treatment, biomarker (dichotomized at quartile 1, median, or quartile 3), interaction of treatment by biomarker, International Federation of Gynecology and Obstetrics (FIGO) stage and debulking status, and baseline performance status as covariates. †Stratified analysis (using the two stratification factors used for patient random assignment: FIGO stage and debulking status, and baseline performance status). BEI = biomarker-evaluable immunohistochemistry; BEV = bevacizumab; CI = confidence interval; CT = chemotherapy; HR = hazard ratio; NR = not reached; OS = overall survival; PFS = progression-free survival; PLA = placebo; Q = quartile.

ARTICLE

of action of bevacizumab, angiogenesis inhibition-induced tumor cell starvation (37). The observed OS improvement in these populations may reflect the benefit of bevacizumab outweighing other confounding factors, such as crossover or multiple additional therapies. Whether these candidate biomarkers will also predict benefit in other tumor types or indications in which bevacizumab is given only concurrently with chemotherapy remains to be determined. MVD probably varies according to the time within the natural disease history. Therefore, in ovarian cancer, it would be interesting to assess whether this relationship with bevacizumab is present for recurrent disease, including platinum-resistant tumors. Additionally, MVD varies according to tumor type. Comparison of four cancer types using the same MVD measuring technique revealed mean MVD of 112 (SD = ±50) vessels/mm^2 for renal cell cancer (22 patients), 76 (SD = ±21) vessels/mm^2 for colorectal cancer (19 patients), 65 (SD = ±30) vessels/mm^2 for glioblastoma (20 patients), and 43 (SD = ±13) vessels/mm^2 for ovarian cancer (21 patients) (31). From a technical perspective, this means that in epithelial ovarian cancer, which has lower intratumoral MVD, fewer ROIs may need to be interrogated for a representative and reliable MVD assessment (30).

Although VEGF-A and its receptors were considered the most obvious candidate biomarkers, previous results for both have been inconsistent across trials and tissue types, and even—as in the present trial—across end points within a single trial (38). Initially, bevacizumab biomarker research focused on plasma biomarkers due partly to the convenience of their potential clinical application. Retrospective analyses in breast, pancreatic, and gastric cancers suggested that plasma (p)VEGF-A might be a promising candidate biomarker (39–41). However, with increased understanding of the effects of bevacizumab and differences in disease biology, it appears that pVEGF-A is not a robust pan-tumor biomarker (42). More recently, the first prospective trial evaluating pVEGF-A in metastatic breast cancer showed no differential bevacizumab treatment effect on PFS according to baseline pVEGF-A levels (43). The hypothesis for pVEGF-A as a potential predictive biomarker has a particularly

weak rationale in the context of postoperative settings. Exploratory correlative analyses of GOG-0218 showed no predictive effect of baseline plasma concentrations of key candidate biomarkers, including pVEGF-A, for bevacizumab efficacy (44,45). An additional complication in GOG-0218 is that all samples were collected after debulking surgery and before chemotherapy, meaning they reflect removal of bulk tumor and the impact of the surgical wound. However, most VEGF-A secreted by tumors (tVEGF-A) is retained in the extracellular matrix and is released to act on endothelial cells only after proteolytic processing (46). As only a fraction of tVEGF-A is proteolytically processed and biologically active, the relationship between tVEGF-A expression levels and VEGF-A activity may not be linear, and thus the right cutoff level for this marker may not be evident a priori. Interestingly, a relatively small subset of patients in GOG-0218 had tumors expressing extremely high levels of tVEGF-A; in these patients, the VEGF-A pathway may be consistently more active (Supplementary Figure 5, available online). In this study, we observed that patients with the highest tVEGF-A levels (highest quartile) seem to derive an OS benefit from bevacizumab treatment. One might speculate that these high expressers may represent the true VEGF-dependent subpopulation.

In conclusion, this retrospective analysis of GOG-0218 identified high MVD and tVEGF-A levels as potential predictive biomarkers for bevacizumab efficacy in newly diagnosed ovarian cancer. These intriguing findings should be considered when designing future trials, and markers such as MVD and tVEGF-A could eventually inform sequencing of approved targeted therapies in specific patient subpopulations.

Funding

This work was supported by the National Cancer Institute (grant numbers NSC #704865 and IND #113912 to the GOG) and Roche/Genentech; biomarker analyses in this report were funded by Roche/Genentech. Support for third-party medical writing assistance for this manuscript was provided by F Hoffmann-La Roche Ltd, Basel, Switzerland.

Notes

This work was presented by Michael J. Birrer at the Gynecologic Cancer Oral Session of the American Society of Clinical Oncology Annual Meeting, 2015.

Study funders were involved in the design, analysis, and interpretation of the biomarker results reported here, but not the collection of the data. The co-corresponding authors, one of whom is a former employee of the funder, were involved in the writing of the manuscript and the final decision to submit the manuscript for publication. We would like to thank all patients and their significant others; the teams of physicians, nurses, and research coordinators at the 363 study sites; and the Gynecologic Oncology Group, National Cancer Institute, and Roche/Genentech for their dedication. Medical writing assistance was provided by Jennifer Kelly, MA (Medi-Kelsey Ltd, Ashbourne, UK), funded by F Hoffmann-La Roche Ltd., Basel, Switzerland.

References

1. Ferrara N, Adamis AP. Ten years of anti-vascular endothelial growth factor therapy. *Nat Rev Drug Discov*. 2016;15(6):385–403.
2. Ferrara N, Gerber HP, LeCouter J. The biology of VEGF and its receptors. *Nat Med*. 2003;9(6):669–676.
3. Ferrara N, Carver-Moore K, Chen H, et al. Heterozygous embryonic lethality induced by targeted inactivation of the VEGF gene. *Nature*. 1996;380(6573):439–442.
4. Chung AS, Ferrara N. Developmental and pathological angiogenesis. *Annu Rev Cell Dev Biol*. 2011;27:563–584.
5. Vasudev NS, Reynolds AR. Anti-angiogenic therapy for cancer: Current progress, unresolved questions and future directions. *Angiogenesis*. 2014;17(3):471–494.
6. Jayson GC, Kerbel R, Ellis LM, Harris AL. Antiangiogenic therapy in oncology: Current status and future directions. *Lancet*. 2016;388(10043):518–529.
7. Burger R, Brady MF, Bookman MA, et al. Incorporation of bevacizumab in the primary treatment of ovarian cancer. *N Engl J Med*. 2011;365(26):2473–2483.
8. Perren TJ, Swart AM, Pfisterer J, et al. A phase 3 trial of bevacizumab in ovarian cancer. *N Engl J Med*. 2011;365(26):2484–2496.
9. Randall L, Burger R, Nguyen H, et al. Outcome differences in patients with advanced epithelial ovarian, primary peritoneal and fallopian tube cancers treated with and without bevacizumab. *Gynecol Oncol*. 2013;130:e33 (abstract 80).
10. Jubb AM, Miller KD, Rugo HS, et al. Impact of exploratory biomarkers on the treatment effect of bevacizumab in metastatic breast cancer. *Clin Cancer Res*. 2011;17(2):372–381.
11. McCarty JH. Glioblastoma resistance to anti-VEGF therapy: Has the challenge been MET? *Clin Cancer Res*. 2013;19(7):1631–1633.
12. Puszta szeri MP, Seelentag W, Bosman FT. Immunohistochemical expression of endothelial markers CD31, CD34, von Willebrand factor, and Fli-1 in normal human tissues. *J Histochem Cytochem*. 2006;54(4):385–395.
13. Wang D, Stockard CR, Harkins L, et al. Immunohistochemistry in the evaluation of neovascularization in tumor xenografts. *Biotech Histochem*. 2008;83(3-4):179–189.
14. Hollingsworth HC, Kohn EC, Steinberg SM, Rothenberg ML, Merino MJ. Tumor angiogenesis in advanced stage ovarian carcinoma. *Am J Pathol*. 1995;147(1):33–41.
15. Macchiarini P, Fontanini G, Hardin MJ, Squartini F, Angeletti CA. Relation of neovascularisation to metastasis of non-small-cell lung cancer. *Lancet*. 1992;340(8812):145–146.
16. Maeda K, Chung YS, Takatsuka S, et al. Tumour angiogenesis and tumour cell proliferation as prognostic indicators in gastric carcinoma. *Br J Cancer*. 1995;72(2):319–323.
17. Raspollini MR, Amunni G, Villanucci A, Baroni G, Boddi V, Taddei GL. Prognostic significance of microvessel density and vascular endothelial growth factor expression in advanced ovarian serous carcinoma. *Int J Gynecol Cancer*. 2004;14(5):815–823.
18. Gasparini G, Bonoldi E, Viale G, et al. Prognostic and predictive value of tumour angiogenesis in ovarian carcinomas. *Int J Cancer*. 1996;69(3):205–211.
19. Li Y, Ma X, Zhang J, Liu X, Liu L. Prognostic value of microvessel density in hepatocellular carcinoma patients: A meta-analysis. *Int J Biol Markers*. 2014;29:e279–e287.
20. Sun HC, Tang ZY, Li XM, Zhou YN, Sun BR, Ma ZC. Microvessel density of hepatocellular carcinoma: Its relationship with prognosis. *J Cancer Res Clin Oncol*. 1999;125(7):419–426.
21. Wang Y, Yao X, Ge J, Hu F, Zhao Y. Can vascular endothelial growth factor and microvessel density be used as prognostic biomarkers for colorectal cancer? A systematic review and meta-analysis. *Sci World J*. 2014;2014:102736.
22. Weidner N, Folkman J, Pozza F, et al. Tumor angiogenesis: A new significant and independent prognostic indicator in early-stage breast carcinoma. *J Natl Cancer Inst*. 1992;84(24):1875–1887.
23. Brauer MJ, Zhuang G, Schmidt M, et al. Identification and analysis of in vivo VEGF downstream markers link VEGF pathway activity with efficacy of anti-VEGF therapies. *Clin Cancer Res*. 2013;19(13):3681–3692.
24. Des Guetz G, Uzzan B, Nicolas P, et al. Microvessel density and VEGF expression are prognostic factors in colorectal cancer. Meta-analysis of the literature. *Br J Cancer*. 2006;94(12):1823–1832.
25. Foernzler D, Delmar P, Kockx M, et al. Tumor tissue based biomarker analysis in NO16966: A randomized phase III study of first-line bevacizumab in combination with oxaliplatin-based chemotherapy in patients with mCRC. *ASCO Gastrointestinal Cancers Symposium*. 2010; (abstract 374).
26. Jubb AM, Hurwitz HI, Bai W, et al. Impact of vascular endothelial growth factor-A expression, thrombospondin-2 expression, and microvessel density on the treatment effect of bevacizumab in metastatic colorectal cancer. *J Clin Oncol*. 2006;24(2):217–227.
27. Hlatky L, Hahnfeldt P, Folkman J. Clinical application of antiangiogenic therapy: Microvessel density, what it does and doesn't tell us. *J Natl Cancer Inst*. 2002;94(12):883–893.
28. ClinicalTrials.gov number NCT00262847. Carboplatin and paclitaxel with or without bevacizumab in treating patients with stage III or stage IV ovarian epithelial, primary peritoneal, or fallopian tube cancer. https://clinicaltrials.gov/ct2/show/NCT00262847.
29. FIGO Cancer Committee. Staging announcement. *Gynecol Oncol*. 1986;25:383–385.
30. Marien KM, Andries L, De Schepper S, Kockx MM, De Meyer GR. AutoTag and AutoSnap: Standardized, semi-automatic capture of regions of interest from whole slide images. *MethodsX*. 2015;2:272–277.

31. Marien KM, Croons V, Waumans Y, et al. Development and validation of a histological method to measure microvessel density in whole-slide images of cancer tissue. *PLoS One*. 2016;11(9):e0161496.
32. Roche Avastin Summary of Product Characteristics 2015. http://www.ema.europa.eu/docs/en_gb/document_library/epar_-_product_information/human/000582/wc500029271.pdf. Accessed May 25, 2016.
33. Collinson F, Hutchinson M, Craven RA, et al. Predicting response to bevacizumab in ovarian cancer: A panel of potential biomarkers informing treatment selection. *Clin Cancer Res*. 2013;19(18):5227–5239.
34. Gourley C, McCavigan A, Perren T, et al. Molecular subgroup of high-grade serous ovarian cancer (HGSOC) as a predictor of outcome following bevacizumab. *J Clin Oncol*. 2014;32(suppl):5s (abstract 5502).
35. Backen A, Renehan AG, Clamp AR, et al. The combination of circulating Ang1 and Tie2 levels predicts progression-free survival advantage in bevacizumab-treated patients with ovarian cancer. *Clin Cancer Res*. 2014;20(17):4549–4558.
36. Zhou C, Clamp A, Backen A, et al. Systematic analysis of circulating soluble angiogenesis-associated proteins in ICON7 identifies Tie2 as a biomarker of vascular progression on bevacizumab. *Br J Cancer*. 2016;115(2):228–235.
37. Ma J, Waxman DJ. Combination of antiangiogenesis with chemotherapy for more effective cancer treatment. *Mol Cancer Ther*. 2008;7(12):3670–3684.
38. Lambrechts D, Lenz HJ, de Haas S, Carmeliet P, Scherer SJ. Markers of response for the antiangiogenic agent bevacizumab. *J Clin Oncol*. 2013;31(9):1219–1230.
39. Miles DW, de Haas SL, Dirix LY, et al. Biomarker results from the AVADO phase 3 trial of first-line bevacizumab plus docetaxel for HER2-negative metastatic breast cancer. *Br J Cancer*. 2013:108(5):1052–1060.
40. Van Cutsem E, Jayson G, Dive C, et al. Analysis of blood plasma factors in the AVITA phase III randomized study of bevacizumab (bev) with gemcitabine-erlotinib (GE) in patients (pts) with metastatic pancreatic cancer (mPC). European Multidisciplinary Cancer Congress; September 23–27, 2011; Stockholm, Sweden. Abstract 803.
41. Van Cutsem E, de Haas S, Kang YK, et al. Bevacizumab in combination with chemotherapy as first-line therapy in advanced gastric cancer: A biomarker evaluation from the AVAGAST randomized phase III trial. *J Clin Oncol*. 2012;30(17):2119–2127.
42. Bais C, Rabe C, Wild N, et al. Comprehensive reassessment of plasma VEGFA (pVEGFA) as a candidate predictive biomarker for bevacizumab (Bv) in 13 pivotal trials (seven indications). *J Clin Oncol*. 2014;32(suppl 5s): (abstract 3040).
43. Miles D, Cameron D, Bondarenko I, et al. Bevacizumab plus paclitaxel versus placebo plus paclitaxel as first-line therapy for HER2-negative metastatic breast cancer (MERiDiAN): A double-blind placebo-controlled randomised phase III trial with prospective biomarker evaluation. *Eur J Cancer*. 2017;70:146–155.
44. Birrer M, Lankes H, Burger R, et al. Biomarker (BM) results from GOG-0218, a phase 3 trial of front-line bevacizumab (BV) + chemotherapy (CT) for ovarian cancer (OC). *Ann Oncol*. 2012;23(suppl 9):ix81–2 (abstract 198P).
45. Wei W, Brady MF, Tsang T-Y, et al. An assessment of the prognostic and predictive associations of 13 angiogenic biomarkers in women with newly diagnosed advanced ovarian cancer treated with chemotherapy with or without bevacizumab. *Mol Cancer Ther*. 2015;14;PR05.
46. Ferrara N. Binding to the extracellular matrix and proteolytic processing: Two key mechanisms regulating vascular endothelial growth factor action. *Mol Biol Cell*. 2010;21(5):687–690.